Co-evolving stability and conformational homogeneity of the human adenosine A_{2a} receptor

Francesca Magnani, Yoko Shibata, Maria J. Serrano-Vega, and Christopher G. Tate†

Medical Research Council, Laboratory of Molecular Biology, Hills Road, Cambridge CB2 0QH, United Kingdom

Communicated by Richard Henderson, Medical Research Council, Cambridge, United Kingdom, May 14, 2008 (received for review February 20, 2008)

Structural studies on mammalian integral membrane proteins have long been hampered by their instability in detergent. This is particularly true for the agonist conformation of G protein-coupled receptors (GPCRs), where it is thought that the movement of helices that occurs upon agonist binding results in a looser and less stable packing in the protein. Here, we show that mutagenesis coupled to a specific selection strategy can be used to stabilize the agonist and antagonist conformations of the adenosine A_{2a} receptor. Of the 27 mutations identified that improve the thermostability of the agonist conformation, only three are also present in the 17 mutations identified that improve the thermostability of the antagonist conformation, suggesting that the selection strategies used were specific for each conformation. Combination of the stabilizing mutations for the antagonist- or agonist-binding conformations resulted in mutants that are more stable at higher temperatures than the wild-type receptor by 17°C and 9°C, respectively. The mutant receptors both showed markedly improved stability in short-chain alkyl-glucoside detergents compared with the wild-type receptor, which will facilitate their structural analysis.

conformational thermostabilization | G protein-coupled receptor | membrane protein

G protein-coupled receptors (GPCRs) represent one of the largest single families of integral membrane proteins in the human genome and bind multifarious ligands that mediate many physiological processes, which explains why GPCRs represent a major proportion of drug targets (1). The binding of an extracellular ligand to a GPCR promotes coupling of the receptor to trimeric G proteins, situated on the intracellular side of the plasma membrane, triggering a signaling cascade. Despite sharing common features such as seven transmembrane helices and conserved signatures in their amino acid sequence (2), the sequence homology between different GPCRs is rather low. Detailed structure determination of GPCRs is therefore required to elucidate the mechanism of receptor activation to improve the design of both agonist and antagonist ligands of medical relevance.

For many years, crystallographic studies of GPCRs were limited to rhodopsin because of its abundance in native sources (retina) and its intrinsic stability in the dark state (3, 4). However, even rhodopsin has been shown to be structurally more dynamic in detergent solution than in lipid bilayers (5), and such flexibility is more pronounced for GPCRs that bind to diffusible ligands. Another obstacle to structural analysis, and especially to the formation of well ordered crystals, arises from the conformational heterogeneity of these receptors (6, 7). The active agonist-bound state of GPCRs is normally found to be intrinsically less stable than the inactive antagonist-bound state, probably reflecting the receptor requirement for higher flexibility in its active state (8). Agonist binding to the receptor triggers the recruitment of G_α protein binding to the intracellular side of the receptor, possibly via a succession of different conformations (7, 9, 10).

Site-directed mutagenesis was used by Bowie and coworkers to improve the stability of two bacterial membrane proteins (11–13). Rhodopsin has also been stabilized by 10°C, although in this case a disulfide bond was engineered between the N terminus and the third extracellular loop based on structural data (14). Recently, we simultaneously improved both the thermostability and conformational homogeneity of a GPCR, the turkey β_1 adrenergic receptor (β_1AR). The stabilized GPCR mutant, β_1AR-m23, was preferentially in an antagonist-bound conformation, and its thermostability was 21°C higher than the wild-type receptor (15), making it similar in stability to dark-state rhodopsin. In the present work, we further extended this approach of "conformational thermostabilization" on the human adenosine A_{2a} receptor (A_{2a}R) and carried out, in parallel, selection for two distinct conformations, the antagonist- and agonist-bound states.

Results

Alanine-Scanning Mutagenesis. Human A_{2a}R can be solubilized in the mild detergent dodecylmaltoside (DDM), and ligand-binding activity is retained at 4°C for many days, although it is much less stable after purification, probably because of the loss of bound lipids (16). The apparent melting temperature (T_m) of wild-type human A_{2a}R solubilized in 2% DDM when assayed with either the agonist [^{3}H]-5′-*N*-ethylcarboxamidoadenosine (NECA) or the antagonist [^{3}H]-ZM241385 is 23°C (data not shown); in this context, the apparent T_m is defined as the temperature at which 50% of the binding activity remains after a 30-min incubation (15). By comparison, in similar conditions, rhodopsin has an apparent T_m of 55°C and turkey β_1AR, 32°C (15). To make the T_m determination for the wild-type A_{2a}R more reproducible under conditions of fluctuating laboratory temperature, we included 10% glycerol upon solubilization, which raised the apparent T_m of the wild-type receptor from 23°C to 30°C.

The construct used in this study, M-A2aTr316-H10, expresses a maltose-binding protein-A_{2a}R fusion protein with a C-terminal 96-residue truncation designed to remove protease-sensitive sites, followed by a His_{10} tag (16). Each residue in A_{2a}R between Pro-2 and Ala-316 was individually mutated to Ala; if the wild-type residue was Ala, then the replacement was Leu. A total of 315 mutants were expressed in *Escherichia coli* and screened for activity in detergent solution before and after incubation at 30°C (Fig. 1). Our goal was to find mutations that would enhance the thermal stability of the receptor preferentially in either an

Author contributions: F.M., Y.S., M.J.S.-V., and C.G.T. designed research; F.M. performed research; Y.S. and M.J.S.-V. contributed new reagents/analytic tools; F.M. analyzed data; and F.M. and C.G.T. wrote the paper.

Conflict of interest statement: R.H. declares a conflict of interest. I had no conflict of interest while the work described in the manuscript was being carried out. However, during the last 9 months, C.G.T. and I have helped to found a small United Kingdom-based company called Heptares Therapeutics Limited, to which the Medical Research Council (MRC) has assigned commercial rights to any work carried out at the MRC Laboratory of Molecular Biology on any G protein-coupled receptor, including the adenosine A2a receptor work reported in the paper. The remaining authors declare no conflict of interest.

†To whom correspondence should be addressed. E-mail: cgt@mrc-lmb.cam.ac.uk.

This article contains supporting information online at www.pnas.org/cgi/content/full/0804396105/DCSupplemental.

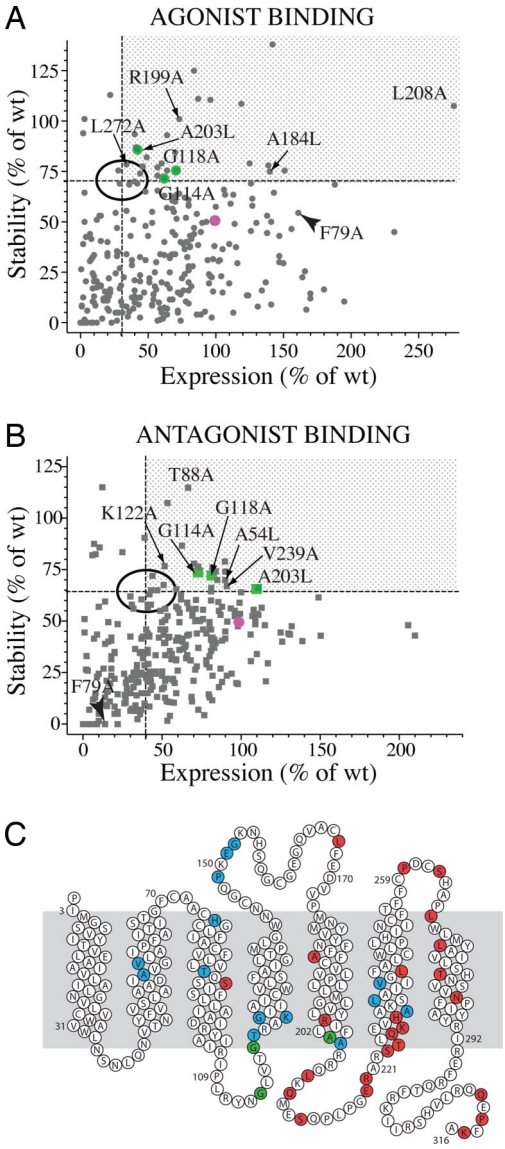

Fig. 1. Activity and thermal stability of $A_{2a}R$ mutants. Stability is measured by the ratio of residual radioligand binding after incubation at 30°C for 30 min to initial activity. Under these conditions, wild-type receptor activity decayed to 50% of its initial value. (*A* and *B*) Data for the mutants were normalized to wild-type activity (pink dot). Expression of each active receptor variant was measured by a single-point binding assay by using either [^{3}H]-NECA (*A*) or [^{3}H]-ZM241385 (*B*). The black ellipse in each plot indicates the standard deviation in activity and stability values. Dashed horizontal and vertical lines indicate the cutoff values used to select for stability and expression levels of the best mutants (gray area, top right). G114A, G118A, and A203L mutants, which were the only ones that increased stability significantly for both agonist and antagonist binding, are indicated in green. The inherent variability of the screen was ± 10%. Mutations that comprise the final stabilized mutants Rag23 and Rant21 are labeled with the residue number. F79A is also marked (see *Results*). (*C*) Snake plot showing the amino acid position of the thermostabilizing mutations (agonist subset in red, antagonist subset in blue, and the three overlapping residues in green).

agonist- or antagonist-binding conformation, preferably without ligand bound, so that ligand-affinity purification could be used for the subsequent production of receptors for crystallization. The stability of the mutants, therefore, was tested by using in parallel both the agonist [^{3}H]-NECA and the antagonist [^{3}H]-ZM241385 after heating the solubilized unliganded receptor. Intuitively, it might be thought that this strategy may not succeed, because of rapid equilibration between R and R* if the receptor behaved as expected to the two-state model: this model states that the receptor in the absence of ligand exists in an equilibrium between a state R that is inactive and does not couple to downstream signaling, and the R* state (agonist-binding state) that can signal. However, for the *E. coli*-expressed $A_{2a}R$, we have not been able to observe any interconversion between the R and R* conformations at 0°C in detergent over a period of 14 h; under these conditions, only one-tenth of binding sites were measured with the agonist [^{3}H]-NECA, compared with the number of binding sites measured by antagonist binding. Consequently, there may have been only very limited interconversion between the R and R* conformations during the 30-min incubation at 30°C used to assay the stability of the receptor. Therefore, [^{3}H]-NECA-binding experiments measured only receptors specifically in the agonist- and not in the antagonist-binding state; conversely, [^{3}H]-ZM241385 measured only receptors in the antagonist- and not the agonist-binding state. An added complexity for $A_{2a}R$ is that Na^+ ions present in the buffer act as an allosteric antagonist [supporting information (SI) Fig. S1 (17, 18)], which shifts the receptor equilibrium toward the R conformation. Despite the many complexities in this thermostability assay, we found this strategy for selecting thermostable mutants was indeed successful.

Levels of expression were estimated by ligand binding, using ligand concentrations 5- to 10-fold above K_D to minimize the impact of possible changes in affinity. When the first round of mutants from the Ala scan was assayed, a mutant with improved stability (≥65% or 70% of residual activity for antagonist or agonist selection, respectively) was accepted only if the expression of active receptor was no less than 30% (agonist selection) or 40% (antagonist selection) that of wild-type $A_{2a}R$ (Fig. 1); there was no significant correlation between thermostability and improved expression. Using these cutoff values, we selected 27 stabilizing mutations by agonist and 17 by antagonist binding (Table S1). The stabilizing point mutations populate two distinct subsets, as defined by agonist or antagonist binding. Only three mutants were found to have a stabilizing effect for both conformations, i.e., G114A, G118A, and A203L (Fig. 1). Thermostabilizing mutations appeared mainly to be residues that are predicted from the rhodopsin structure to be exposed either to the lipid or the aqueous environment (27 residues in total; Table S1), although some (10 residues) appeared to be partially buried, and the remaining seven residues were predicted to be totally buried. Ten of the 27 mutations that stabilized the agonist-binding conformation were found either in the third intracellular loop or at the putative cytoplasmic end of helix 6 (Fig. 1*C*).

Combining Mutations. Thermostabilizing mutations can be additive (11, 15), so we assembled some of the best mutations identified in the initial screening into individual mutant receptors. The goal was to improve simultaneously the receptor stability in detergent solution and its conformational homogeneity in either an agonist or antagonist conformation. The second generation of mutants was therefore synthesized by combining stabilizing mutations for each specific conformation (Table S1). The combination of clusters of adjacent mutations (Table S1, boxed) often resulted in receptor variants that were less thermostable than the single mutants, as was also found for turkey β_1AR (15). From this second round of mutagenesis, the most thermostable combinations obtained were R*ag*1 (A184L+R199A+L272A) and R*ant*5 (A54L+T88A+V239A), as determined by agonist or antagonist binding, respectively. Compared with the wild-type receptor, Rag1 showed an increase in apparent T_m of 5°C both in the unliganded and agonist-occupied state, whereas the T_m of Rant5 was 11°C and 14°C higher than for the wild-type receptor for the unliganded and antagonist-occupied state, respectively.

BIOCHEMISTRY

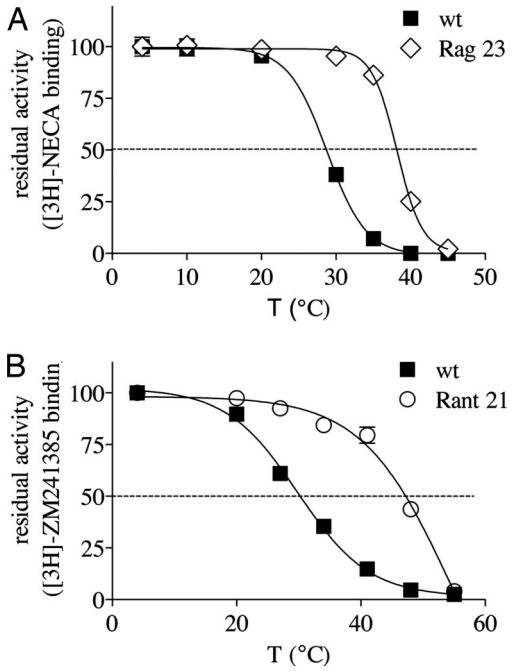

Fig. 2. Thermostability of wild-type receptor and mutants Rag23 and Rant21 in the presence of the appropriate bound [^{3}H]-ligand. Detergent-solubilized receptors were preincubated with either (*A*) agonist [^{3}H]-NECA or (*B*) antagonist [^{3}H]-ZM241385, followed by incubation at the temperatures indicated for 30 min. Wild-type (dark squares) and mutants (open diamonds, Rag23, and open circles, Rant21). Data points are from duplicate measurements and are representative of three independent experiments.

To explore the possibility of further stabilization, Rag1 and Rant5 were subjected to one-third round of mutagenesis. Of many combinations screened, we identified Rag23 (F79A, A184L, R199A, L208A, L272A) and Rant21 (A54L, T88A, K122A, V239A) as the most thermostable variants, with a 9°C and 17°C, respectively, increase in the apparent T_m of the ligand-occupied state, compared with wild type (Fig. 2 and Table S2). A list of the receptor variants generated in the second and third round of mutagenesis is given in Table S3.

Saturation Curves and Competition Assays. To characterize the conformational identity of the thermostable mutants, we carried out saturation-binding and competition assays using several agonist and antagonist ligands (Table S4 and Fig. 3). During the generation of a thermostable antagonist-binding conformation of $A_{2a}R$, the majority of combinations created in the second and third rounds of mutagenesis displayed saturable antagonist binding ([^{3}H]-ZM241385) but were no longer capable of binding the agonist [^{3}H]-NECA (Fig. 3*A*). The most stable mutant of this subset, Rant21, bound [^{3}H]-ZM241385 with a K_D value of 15 nM, and two other antagonists, xanthine amine congener (XAC) and theophylline, had K_i values of 2.1 μM and 0.86 mM, respectively (Fig. 3 *B–D*); these values are all close to the wild-type values obtained ([^{3}H]-ZM241385, K_D 12 nM; XAC, K_i 2.3 μM; theophylline, K_i 1.5 mM). However, the affinity of Rant21 for agonists was weaker; for [^{3}H]-NECA, the K_D is >14 times higher, and for (R)-N6-(1-methyl-2-phenylethyl)adenosine (R-PIA), the K_i is 225 times higher than wild type (Table S4 and Fig. 3). Sodium acts as an allosteric antagonist of agonist binding to $A_{2a}R$ (Fig. S1 and refs. 17 and 18) and was therefore omitted in the saturation-binding assay to measure the K_D of [^{3}H]-NECA shown in Fig. 3*A* and Table S4, but it was included in the competition curves using agonists to displace antagonists (Table 1 and Fig. 3 *E* and *F*). This may account for the weaker affinity values for NECA in the competition assay, compared with the saturation-binding assay. Affinity values of wild-type and mutant receptors for both ligands are summarized in Table 1 and Table S4, obtained from data plotted in Fig. 3.

Combining stabilizing mutations for the agonist-binding con-

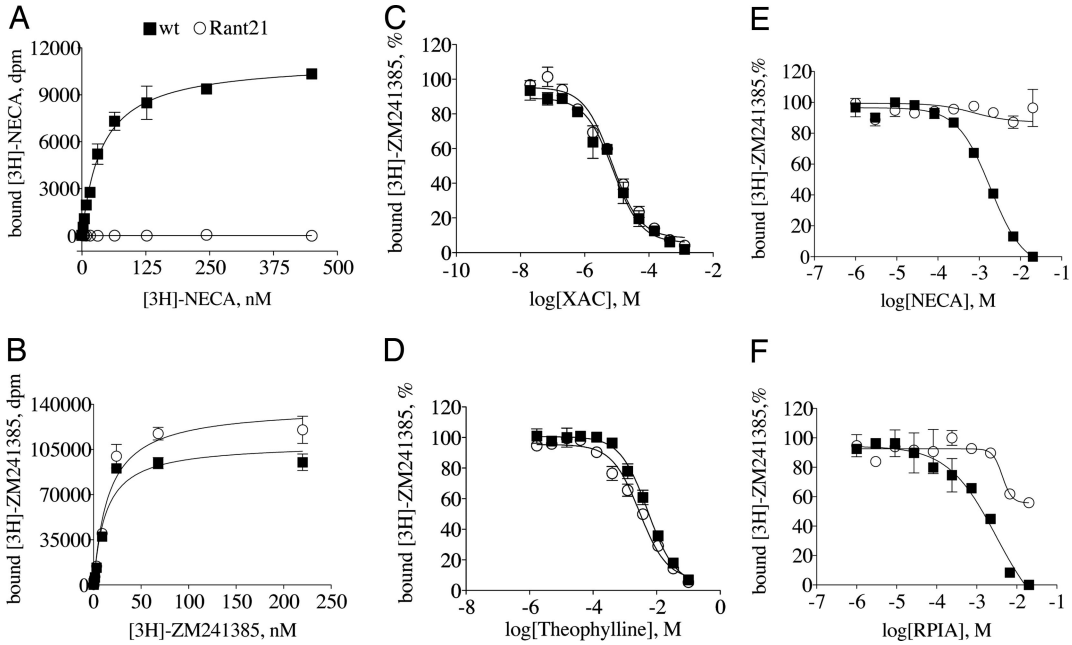

Fig. 3. Pharmacological profile of mutant Rant21. Saturation binding of (*A*) agonist and (*B*) antagonist to solubilized receptors: wild-type $A_{2a}R$, filled squares; Rant21, open circles. (*C–F*) Inhibition of [^{3}H]-ZM241385 binding by increasing concentrations of the antagonists XAC (*C*) and theophylline (*D*) and the agonists NECA (*E*) and RPIA (*F*); wild-type $A_{2a}R$, filled squares; Rant21, open circles. Binding of [^{3}H]-ZM241385 (10 nM) in the absence of unlabeled ligand was set to 100%. Each solubilized receptor was incubated with ligands for 1 h on ice in binding buffer (50 mM Tris, pH 7.5, and 0.025% DDM) either in the presence (400 mM; *A*, *C–F*) or absence of NaCl (*B*). Data shown are from two independent experiments with each data point measured in triplicate. K_D and K_i values are given in Tables 1 and S4.

Table 1. Inhibitor binding to detergent-solubilized wild-type $A_{2a}R$ and Rant21

Competitor	K_i, mM	
	Wild type	Rant 21
XAC	0.002	0.002
Theophylline	1.52 ± 0.05	0.86 ± 0.09
NECA	7.0 ± 0.5	>>20
R-PIA	0.16 ± 0.1	30 ± 16

Assays were carried out as described in *Material and Methods*. Incubation of samples with ligands was for 1 h on ice with [^{3}H]-ZM241385 at a concentration of 10 nM. K_i values were calculated according to the Cheng and Prusoff equation with a K_D for [^{3}H]-ZM241385 of 12 nM (wild-type receptor) and 15 nM (Rant 21 mutant). Values are representative of two independent experiments. Each data point was assayed in triplicate and plotted as mean ± SD (SD is not shown when is < 1% of the mean value).

formation led to receptor variants still capable of binding to both agonist and antagonist ligands (data not shown). Further combinations were therefore screened to make Rag23; the mutation F79A was included in Rag23, despite not being thermostabilizing, because the data from the original screen suggested it was preferentially in the agonist-binding conformation (Fig. 1 *A* and *B*). Further work subsequently showed that these binding data arose because of F79A being less sensitive to the allosteric antagonism of Na^+ (results not shown). The inclusion of F79A mutation fits with our goal, because Rag23, when compared with the parental mutant Rag1, showed both enhanced thermostability (an additional 4°C in the ligand-occupied state; Table S2) and 5-fold reduced affinity for the antagonist [^{3}H]-ZM241385 compared with the wild type (Table S4).

Increased Thermostability Correlates with Independence from Lipids. Purification of the wild-type $A_{2a}R$ required the inclusion of cholesteryl hemisuccinate (CHS) and glycerol to maintain its ligand-binding activity (16). From our observations, we found that CHS increases the size of the detergent-lipid micelle around a membrane protein, and we hypothesize that the major stabilization effect of CHS is due to the retention of lipids around the protein. This is equivalent to adding additional lipids to the detergent during purification, which also has a stabilizing effect (19–21). We therefore probed the stability of some of the Rant mutants by varying the concentration of DDM or lipids at a fixed concentration of receptor. The enhanced stability of receptor variants was measurable not only by an increased survival in DDM solution (Fig. 4*A*) but also by a reduced requirement for lipids during purification (Fig. 4*B*).

We then tested whether the increase in receptor thermostability had widened the detergent range we could use for purification and subsequently crystallization (Table 2). Solubilization of the receptor was carried out with 1% DDM, and detergent exchange was performed after immobilization of the receptor via its His_{10} tag to Ni^{2+}-affinity resin. In general, there was a direct correlation between receptor stability and the alkyl chain length of detergents (Table 2). Surprisingly, the antagonist-binding conformation of the wild-type receptor was less stable in shorter chained maltoside detergents than the agonist-binding state yet another reflection of the structural differences between the two states. Thus, the increased stability of the $A_{2a}R$ mutants has removed the requirement of additional lipids during purification to maintain the activity of the receptor and will allow a larger range of detergents to be used during crystallization.

Discussion

GPCRs represent a challenge for structural studies, because they are often rapidly inactivated upon solubilization in detergent,

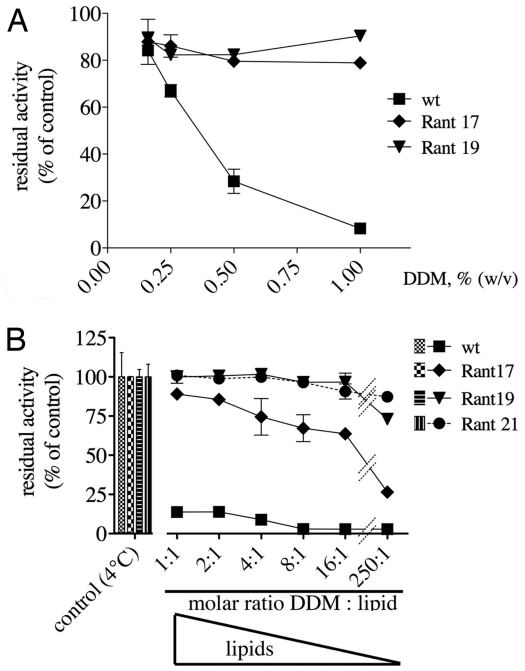

Fig. 4. Rant mutants are more stable than wild-type $A_{2a}R$ in the absence of lipids. Thermostable mutants show an increased survival at higher concentration of DDM (*A*) and a decreased dependence on added *E. coli* phospholipids (*B*) upon heating at 35°C for 30 min compared with the wild-type receptor. Receptors were solubilized in 1% DDM (diluted in 50 mM Tris, pH 7.5, and 400 mM NaCl) and immobilized on Ni-NTA agarose for the immobilized metal ion affinity chromatography (IMAC) step. Exchange of buffer containing 0.025% DDM (final) and the appropriate concentration of lipids (0.25, 0.125, 0.06, 0.03, 0.015, and 0 mg/ml) was performed during washes and elution from the Ni-NTA beads.

and also because each receptor exists in at least two, and possibly multiple, conformational states (6). In addition, the agonist-bound state of GPCRs is frequently found to be less stable than the antagonist-bound state (8) making it even more difficult to crystallize. The two GPCR structures so far determined by x-ray crystallography represent conformations close to the antagonist-bound state, and both of these proteins, rhodopsin and the human β2 adrenergic receptor (4, 22, 23), are among the most stable GPCRs. In contrast, $A_{2A}R$ is rapidly inactivated when purified in DDM unless stabilizing agents such as cholesteryl hemisuccinate are present throughout (16).

In this study, we have used the technique of conformational thermostabilization (15) to generate two variants of the human $A_{2a}R$ that correspond to the agonist- and antagonist-binding

Table 2. Stability of wild-type and mutant receptors in different detergents

	Apparent T_m, °C			
	Agonist binding		Antagonist binding	
	Wild type	Rag 23	Wild type	Rant 21
Dodecylmaltoside	27	34	25	39
Decylmaltoside	23	29	10	28
Nonylmaltoside	22	28	<4	25
Nonylglucoside	*	*	*	22
Octylglucoside	<9	16	*	23

Solubilization of receptors and detergent exchange was performed during the IMAC step as described in Fig. 3. SD is <1°C.
*No detectable binding of the radioligand.

BIOCHEMISTRY

conformations. The initial alanine scan identified 17 thermostabilizing mutations for the antagonist- and 27 for the agonist-binding conformation, and the two patterns were largely nonoverlapping (Fig. 1), suggesting that the different mutations stabilize two different states of the receptor. In a second round of mutagenesis, combinations of single thermostable mutants were combined, tested for expression levels and thermostability, and then further refined in a third round. For the generation of an $A_{2A}R$ mutant in the antagonist conformation, this process progressed linearly, with the contribution of single mutations usually being additive and simultaneously increasing the thermostability of both the unliganded and antagonist-bound conformations. This process resulted in the mutant Rant21, which is more stable in both the unliganded and antagonist-occupied states by 10°C and 17°C, respectively, relative to the wild type (Table S2). Generation of the $A_{2a}R$ mutant in the agonist-binding conformation was less straightforward; for example, a single mutation might increase the thermostability of the agonist-occupied state, but not necessarily the stability of the unliganded R* state. It is possible that different mutations affected differentially multiple states of the receptor within the agonist-binding population (7), which resulted in the difficulty of assembling multiple mutations into a single highly stable receptor in an agonist conformation (further work, in progress, is still required to improve the selection procedure of specific agonist binding states). The best agonist-binding mutant obtained so far was Rag23, which displayed a thermostability increase of 9°C in its agonist-occupied state, but it is more stable than the wild type by only 1°C in the unliganded state (Table S2). This represents a substantial 27-fold increase in thermostability of the agonist-occupied state and a significant improvement in stability in short-chain detergents (Table 2).

The pharmacological profile of Rant21 showed that the mutant receptor bound the antagonists ZM241385, XAC, and theophylline with similar affinities compared with the wild-type receptor. In contrast, binding to agonists was dramatically reduced, with the affinity for R-PIA and [^{3}H]-NECA being weakened by at least a factor of 225- and 14-fold, respectively (Table 1 and Table S4). This could suggest that the mutations in Rant21 have a global effect on the receptor structure, so that it preferentially adopts an antagonist-bound conformation. An alternative explanation is that the mutations are all in the ligand-binding pocket, and that coincidentally they specifically inhibit agonist binding, leaving antagonist binding unaffected (see also next paragraph). Mapping the mutations to the recently solved structure of the β_2 adrenergic receptor (refs. 22 and 23 and Fig. S2) shows that K122 and A54 are both predicted to point into the lipid bilayer, V239 is at the interface between helices, and T88 is predicted to be in the ligand-binding pocket (24). It is conceivable that at least part of the weakening of agonist binding could be due to a direct reduction in the agonist affinity through removal of either hydrogen bond(s) or hydrophobic contacts. The structure of Rant21 with antagonist bound would thus be extremely informative regarding the inactive state of the receptor, as has been found in the case of the rhodopsin and β_2AR structures. However, none of these structures is particularly illuminating about the agonist-bound state, because of the receptor conformational change that is predicted to occur upon agonist binding; this will necessitate the structure determination of receptors stabilized specifically in this activated state.

The mutant Rag23 contains five mutations that increase the thermostability of the $A_{2a}R$ only when agonist is bound. Saturation-binding curves for the agonist [^{3}H]-NECA show that Rag23 binds it with marginally stronger affinity than the wild-type receptor; in contrast, binding of the antagonist [^{3}H]-ZM214385 was 5-fold weaker than wild type (Table S4). The positions of these mutations include two predicted to point into the lipid bilayer (F79A and L272A), with another two predicted to be at the interface between transmembrane helices (A184L and R199A), whereas the mutation at L208 is predicted to be in the connecting loop between helices 5 and 6 (inner loop 3; Fig. S2). It is therefore likely that stabilization of the $A_{2a}R$ in the agonist-bound conformation is due primarily to a global shift in structure as opposed to side chain–ligand interactions. We found it much more difficult to assemble the individual mutations that thermostabilize the agonist conformation compared with the combination of mutations to make the antagonist-stabilized Rant21. This may be partly due to the presence of multiple agonist conformations that differ in the degree of conformational change, such as has been proposed for the different effects of partial and full agonists (25). In addition, the proposed conformational change, which is thought to be predominantly an outward movement of helix 6 (26), may result in a more open structure that is more difficult to stabilize than the compact antagonist-bound conformation. The modest increase in stability of Rag23 compared with wild-type $A_{2a}R$ relative to the stabilization of the antagonist conformations of both $A_{2a}R$ and β_1AR (15) is probably a reflection of both these factors.

The $A_{2a}R$ is now the second receptor that we have thermostabilized by alanine-scanning mutagenesis, so we were naturally very interested to examine whether there was any correlation in the residues the procedure selected. A comparison of the thermostabilizing mutations for the β_1AR (15) and for the antagonist conformation of $A_{2a}R$ shows that there is little commonality between their positions in an alignment of the receptors. It may be that this is merely a reflection of their lack of homology, because they are only 23% identical, despite the expectation that the packing of the transmembrane α-helices would be very similar. In contrast, there is thought to be a substantial change in the orientation of at least helix 6 when agonists bind to GPCRs, so it is perhaps not surprising that there were only 3-aa residues that were identified as stabilizing the receptor in both the agonist and antagonist conformations, of 27 and 17 stabilizing mutations, respectively.

The properties of the two thermostabilized $A_{2a}R$ mutants, Rant21 and Rag23, make them attractive for crystallization. Both mutants show a wider range of stability in the short-chain detergents that are preferred for crystallization than the wild-type receptor. Further experiments showed two important changes conferred on mutated receptors by thermostabilization. First, the mutant is significantly less sensitive to elevated detergent concentrations, and second, there is no longer a dependence upon the presence of lipids during purification to maintain ligand-binding activity. The removal of this lipid dependence now allows the preparation of Rant21 in small well defined detergent micelles that should facilitate the formation of well ordered crystals.

Materials and Methods

Materials. The construct M-A2aTr316-H10 in the *E. coli* expression vector pRG/III-hs-MBP used for site directed-mutagenesis was kindly provided by Markus Weiss (Novartis) and is described in ref. 16. NECA was supplied by Amersham Biosciences and [^{3}H]-ZM241385 by American Radiolabeled Chemicals. X AC, R-PIA, NECA, and theophylline were purchased from Sigma. ZM241385 was from Tocris. Ni-nitrilotriacetic acid (Ni-NTA) agarose was obtained from Qiagen and Sephadex G-25 medium from Amersham Biosciences. All detergents were from Anatrace.

Mutagenesis. Mutants were generated by PCR using the QuikChange II methodology (Stratagene) and the expression plasmid as template. PCRs were transformed into DH5α ultracompetent cells prepared according to the Inoue method (27), and individual clones were fully sequenced to check that only the desired mutation was present. Different mutations were combined by PCR as above by (*i*) designing pairs of oligonucleotides to include two to four multiple mutations (Table S1, residues boxed in bold) or (*ii*) randomly, by including in the same PCR mix all of the pairs of primers that introduced the desired

mutations. Several clones were then sequenced from each reaction to determine exactly which mutations were introduced.

Protein Expression. DH5α cells were used to express A_{2a}R and its mutants, as described by Weiss and Grisshammer (16). Briefly, cultures of 500 ml of 2× TY medium supplemented with ampicillin (100 μg/ml), glucose (0.2%, wt/vol), and theophylline (100 μM) were grown at 37°C with shaking. At OD_{600} ≈0.7, the temperature was reduced to 20°C, and IPTG was added to a final concentration of 0.5 mM. Cells were harvested 24 h later by centrifugation at 13,000 ×*g* for 1 min (aliquots of 2 ml) and stored at −20°C (the typical final cell density was OD_{600} = 5.5–6).

Ligand-Binding Assay on Crude Solubilisate. For the assays, cells were resuspended in 250 μl of ice-cold buffer A [50 mM Tris, pH 7.4; 0.4 M NaCl, and protease inhibitors (Complete, Roche)] supplemented with 100 μg/ml lysozyme and DNase I (Sigma). After incubation for 1 h at 4°C, samples were sonicated for 1 min at 4°C in a Misonix 3000 cup-horn sonicator (60 W). Samples were then solubilized with 2% DDM plus 10% glycerol in buffer A on ice for 1 h. Glycerol was included to attain a reproducible baseline for the wild-type receptor. Insoluble material was removed by centrifugation (15,000 ×*g*, 5 min, 4°C), and the supernatant was used directly in radioligand-binding assays.

Partial Purification for Detergent Exchange. For competition assays, and to test different detergents or lipids, pellets from 14 ml of each culture were solubilized in 800 μl of buffer A containing 1% DDM, lysed as above, and then partially purified with Ni-NTA agarose (Qiagen). Ni-NTA agarose (300 μl) was added to 700-μl solubilized samples in buffer A containing 5 mM imidazole, pH 7.4, and 0.025% DDM and incubated for 3 h at 4°C. After incubation, samples were centrifuged at 13,000 ×*g* for 10 seconds at 4°C and washed three times with 1 ml of buffer A for antagonist binding or buffer B (50 mM Tris, pH 7.4, and protease inhibitors) for agonist binding, supplemented with 5 mM imidazole and 0.025% DDM. If necessary, detergent exchange was performed during the washing step; detergent concentrations used for the washing and elution steps were as follows: 0.01% dodecylmaltoside, 0.1% decylmaltoside, 0.3% nonylmaltoside, 0.3% nonylglucoside, and 0.6% octyl glucoside. Receptors were finally eluted in 700 μl of buffer A or B, containing 50 mM histidine plus the relevant detergent.

Radioligand-Binding and Thermostability Assays. Single-point binding assays on solubilized cells contained 50 mM Tris, pH 7.4; 0.4 M NaCl; 10% glycerol; and 2% DDM with 4 μM NECA ([^{3}H]-NECA was diluted with cold ligand to a final concentration of 4 μM in a 1:10 molar ratio) or 500 nM [^{3}H]-ZM241385 in a final volume of 120 μl; equilibration was for 1 h at 4°C. Thermostability was assessed by incubating the binding assay mix, with or without radioligands, at the specified temperature for 30 min; reactions were placed on ice and radioligands added as necessary and equilibrated for an additional 1 h. Receptor-bound and free radioligand were separated by gel filtration as described in ref. 28. Nonspecific binding was determined in parallel on DH5α cells that did not express the receptor. Saturation-binding curves were obtained by using a range of radioligand concentration as indicated in *Results*. Competition assays were performed by using a concentration of [^{3}H]-ZM241385 of 12 nM for wild-type A_{2a}R and 15 nM for the Rant21 mutant (corresponding to their respective K_D values for the ligand) and various concentrations of unlabeled ligands, as indicated. Radioactivity was counted on a Beckman LS6000 liquid scintillation counter, and data were analyzed by nonlinear regression using Prism software (GraphPad).

ACKNOWLEDGMENTS. We are grateful to R. Henderson for invaluable support and comments throughout this study. We are indebted to V. Korkhov, K. R. Vinothkumar, G. F. Schertler (Medical Research Council Laboratory of Molecular Biology, Cambridge, U.K.), and members of the G. F. Schertler's laboratory for critical discussion. We thank M. Weiss (Novartis) and R. Grisshammer (National Institute of Neurological Disorders and Stroke, National Institutes of Health) for plasmid constructs and informal discussions about previously published work. This work was supported by the Medical Research Council Technology Development Gap Fund and Pfizer.

1. Hopkins AL, Groom CR (2002) The druggable genome. *Nat Rev Drug Discov* 1:727–730.
2. Baldwin JM (1994) Structure and function of receptors coupled to G proteins. *Curr Opin Cell Biol* 6:180–190.
3. Li J, Edwards PC, Burghammer M, Villa C, Schertler GF (2004) Structure of bovine rhodopsin in a trigonal crystal form. *J Mol Biol* 343:1409–1438.
4. Palczewski K, *et al.* (2000) Crystal structure of rhodopsin: A G protein-coupled receptor. *Science* 289:739–745.
5. Kusnetzow AK, Altenbach C, Hubbell WL (2006) Conformational states and dynamics of rhodopsin in micelles and bilayers. *Biochemistry* 45:5538–5550.
6. Christopoulos A, Kenakin T (2002) G protein-coupled receptor allosterism and complexing. *Pharmacol Rev* 54:323–374.
7. Kobilka BK, Deupi X (2007) Conformational complexity of G-protein-coupled receptors. *Trends Pharmacol Sci* 28:397–406.
8. Gether U, *et al.* (1997) Structural instability of a constitutively active G protein-coupled receptor. Agonist-independent activation due to conformational flexibility. *J Biol Chem* 272:2587–2590.
9. Ghanouni P, *et al.* (2001) Functionally different agonists induce distinct conformations in the G protein coupling domain of the beta 2 adrenergic receptor. *J Biol Chem* 276:24433–24436.
10. De Grip WJ (1982) Thermal stability of rhodopsin and opsin in some novel detergents. *Methods Enzymol* 81:256–265.
11. Lau FW, Nauli S, Zhou Y, Bowie JU (1999) Changing single side-chains can greatly enhance the resistance of a membrane protein to irreversible inactivation. *J Mol Biol* 290:559–564.
12. Faham S, *et al.* (2004) Side-chain contributions to membrane protein structure and stability. *J Mol Biol* 335:297–305.
13. Zhou Y, Bowie JU (2000) Building a thermostable membrane protein. *J Biol Chem* 275:6975–6979.
14. Standfuss J, *et al.* (2007) Crystal structure of a thermally stable rhodopsin mutant. *J Mol Biol* 372:1179–1188.
15. Serrano-Vega MJ, Magnani F, Shibata Y, Tate CG (2008) Conformational thermostabilisation of the β-adrenergic receptor in a detergent resistant form. *Proc Natl Acad Sci USA* 105:877–882.
16. Weiss HM, Grisshammer R (2002) Purification and characterization of the human adenosine A(2a) receptor functionally expressed in *Escherichia coli*. *Eur J Biochem* 269:82–92.
17. Ji XD, Jacobson KA (1993) Solubilized rabbit striatal A2a-adenosine receptors: Stability and antagonist binding. *Arch Biochem Biophys* 305:611–617.
18. Gao ZG, Jiang Q, Jacobson KA, Ijzerman AP (2000) Site-directed mutagenesis studies of human A(2A) adenosine receptors: Involvement of glu(13) and his(278) in ligand binding and sodium modulation. *Biochem Pharmacol* 60:661–668.
19. Guan L, Smirnova IN, Verner G, Nagamori S, Kaback HR (2006) Manipulating phospholipids for crystallization of a membrane transport protein. *Proc Natl Acad Sci USA* 103:1723–1726.
20. Palsdottir H, Hunte C (2004) Lipids in membrane protein structures. *Biochim Biophys Acta* 1666:2–18.
21. Yao Z, Kobilka B (2005) Using synthetic lipids to stabilize purified beta2 adrenoceptor in detergent micelles. *Anal Biochem* 343:344–346.
22. Rasmussen SG, *et al.* (2007) Crystal structure of the human beta(2) adrenergic G-protein-coupled receptor. *Nature* 450:383–387.
23. Cherezov V, *et al.* (2007) High-resolution crystal structure of an engineered human {beta}2-adrenergic G protein coupled receptor. *Science* 318:1258–1265.
24. Jiang Q, *et al.* (1996) Hydrophilic side chains in the third and seventh transmembrane helical domains of human A2A adenosine receptors are required for ligand recognition. *Mol Pharmacol* 50:512–521.
25. Seifert R, Wenzel-Seifert K, Gether U, Kobilka BK (2001) Functional differences between full and partial agonists: evidence for ligand-specific receptor conformations. *J Pharmacol Exp Ther* 297:1218–1226.
26. Knierim B, Hofmann KP, Ernst OP, Hubbell WL (2007) Sequence of late molecular events in the activation of rhodopsin. *Proc Natl Acad Sci USA* 104:20290–20295.
27. Inoue H, Nojima H, Okayama H (1990) High efficiency transformation of *Escherichia coli* with plasmids. *Gene* 96:23–28.
28. Warne T, Chirnside J, Schertler GF (2003) Expression and purification of truncated, non-glycosylated turkey beta-adrenergic receptors for crystallization. *Biochim Biophys Acta* 1610:133–140.